Supporting Information

Unusual ceria dispersion formed in confined space: a stable and reusable adsorbent for aromatic sulfur capture

Yu Yin, Ding-Ming Xue, Xiao-Qin Liu*, Ge Xu, Peng Ye, Mei-Yan Wu and Lin-Bing Sun*

State Key Laboratory of Materials-Oriented Chemical Engineering, College of Chemistry and Chemical Engineering, Nanjing University of Technology, Nanjing 210009, China

* Corresponding author. E-mail: liuxq@njut.edu.cn; lbsun@njut.edu.cn.

Experimental Section

Materials Synthesis.

Mesoporous silica SBA-15 was synthesized according to the procedure reported by Zhao *et al.*[1] Two gram of Pluronic P123 was first dissolved in 75 g of HCl aqueous solution (1.6 M). Then 4.25 g of silica source tetraethylorthosilicate (TEOS) was added and stirred at 40 ^{o}C for 24 h, followed by hydrothermal treatment at 100 ^{o}C for 24 h. The as-prepared sample was recovered by filtration and dried at the room temperature. Thermogravimetric (TG) analysis shows a weight loss of 50% below 600 ^{o}C, due to the decomposition of template. This is consistent with the reported value (52%),[2] indicating that the template is maintained in the pores of as-prepared SBA-15. The removal of template was conducted by calcination at 550 ^{o}C for 5 h in flowing air.

The precursor $Ce(NO_3)_3{\cdot}6H_2O$ was introduced to as-prepared SBA-15 *via* solid-state grinding at ambient conditions for 30 min. The thoroughly mixed powder was calcined in flowing air at 500 ^{o}C for 5 h to form active species CeO_2 and remove template simultaneously. The obtained composites were denoted as *x*CeAS, where *x* represents the content of CeO_2 in SBA-15 (mol%). In a similar process, *x*CeCS samples were prepared by introducing CeO_2 to calcined SBA-15 without template.

The reference sample CuCl-modified SBA-15 (CuCl/SBA-15) was prepared according to the reported method.[3,4] Four mmol of CuCl and 1.0 g of SBA-15 were extensively mixed and solid-state ground for 30 min. The resulting powder was then thermally treated at 380 ^{o}C for 2 h in dry Ar atmosphere to disperse CuCl. A mechanical mixture of CeO_2 and SBA-15 was also prepared and denoted as 1.5CeO_2-SBA-15. The sample has the same Ce content as 1.5CeAS.

Characterization.

X-ray diffraction (XRD) patterns of the meterials were recorded on a Bruker D8 Advance diffracto-meter with Cu K_{α} radiation in the 2θ ranges from 0.7^{o} to 6^{o} (for low-angle patterns) and 5^{o} to 70^{o} (for high-angle patterns) at 40 kV and 40 mA. Transmission electron microscopy (TEM) was performed on a JEM-200CX electron microscope operated at 200 kV. The N_2 adsorption-desorption isotherms were measured using an ASAP2020 system at −196 °C. Prior to analysis, the samples were evacuated at 200 °C for 4 h. For the samples containing template, the pretreatment was conducted at 50 °C for 2 h to avoid the possible decompsoition of tempalte.[5] The Brunauer-Emmett-Teller (BET) surface area was calculated using the adsorption branch in the relative pressure range from 0.04 to 0.20. The total pore volume was derived from the amount adsorbed at the relative pressure of about 0.99. The pore size distributions were calculated by Barrett-Joyner-Halenda (BJH) method according to the adsorption branch.

Fourier transform infrared (IR) spectra were recorded on a Nicolet Nexus 470 spectrometer with a spectra resolution of 2 cm^{-1} using transparent KBr pellets. Diffuse reflectance UV-vis spectroscopy was carried out on the Perkin Elmer Lambda 950 spectrometer. Thermogravimetric (TG) analysis was performed on a thermobalance (STA-499C, NETZSCH). About 10 mg of sample was heated from the room temperature to 800 °C in a flow of air (25 $mL \cdot min^{-1}$).

Adsorptive Test.

The model fuel was prepared by mixing thiophene, benzothiophene (BT) or 4,6-dimethyldibenzothiophene (DMDBT) with isooctane, and the sulfur concentration was measured to be 550, 560, and 506 ppmw (parts per million by weight), respectively. The desulfurization capacity of materials was evaluated on the basis of breakthrough curves. Experiments were performed in a vertical quartz column with a supporting quartz grid. All adsorptive tests were conducted at the room temperature. The testing fuel was pumped up with a mini creep pump. After the adsorbents were activated *in situ*, the feed was switched to the model fuel and the feed rate was kept at 3$mL \cdot h^{-1}$. Effluent solutions were collected at regular intervals until saturation was reached. The sulfur content in effluent solutions was determined with a Varian 3800 gas chromatograph (GC) equipped with a pulsed-flame photometric detector (PFPD). A calibration curve was prepared to analyze the GC results. Breakthrough curves were generated by plotting the normalized sulfur concentration versus the cumulative fuel volume. The normalized concentration (c/c_0) was obtained from the detected content (c) divided by the initial content (c_0), and the cumulative fuel volume was normalized by the adsorbent weight. The adsorption capacity was calculated by integral calculus as shown in Eq. 1.

$$q = \frac{v}{m}\frac{\rho X_0}{M}\int_0^t (1 - \frac{c_t}{c_0})dt \qquad (1)$$

Where q is the total sulfur adsorbed amount (mmol·g^{-1}), v is the feed volumetric flow rate (mL·min^{-1}), ρ is the fuel density (g·mL^{-1}) at room temperature, X_0 is the total sulfur fraction (by weight) in the feed, c_0 is the total sulfur concentration in the feed (ppmw), m is the weight of the sorbent bed (g), M the molecular weight of sulfur (g·mol^{-1}), c_t the effluent total sulfur concentration (ppmw) at time t (min). The integral on the right hand side of Eq. 1 is the area above the breakthrough curves at any time t. The adsorption capacity mentioned in the present study was calculated at saturation; at that time the effluent sulfur concentration was equal to the sulfur concentration in the feed.

For competitive adsorption, 10 wt% of *tert*-butyl benzene was added to the aforementioned model fuel. The adsorptive desulfurization was conducted similar to the process described above. Regeneration of the adsorbents was carried out *in situ*. For CeAS samples, the used adsorbents were swept with air at the room temperature for 12 h, followed by heating in flowing air at 500 °C for 5 h. For the regeneration of CuCl/SBA-15, the used adsorbent was swept with Ar at room temperature for 12 h, followed by heating in flowing Ar at 380 °C for 2 h.[4,6] After cooling to the room temperature, the regenerated adsorbents were employed for desulfurization again. The long-time stability of adsorbents was assessed by exposing the samples to ambient conditions, where active sites may interact with moisture and oxygen in atmosphere. After a certain period of time (7-45 days), the sample was employed for adsorptive desulfurization.

Supplementary Results and Discussion

Solid-State Grinding and Confined Space.

The solid-state grinding method has already been employed for the introduction of guest to mesoporous silica. This method has been reported to be more effective to disperse oxide than impregnation.[7] In the case of impregnation, the competition from the solvent may hinder the adsorption of guest species.[8] For the solid-state grinding method, there is no competition from solvent molecules; therefore guest is easy to interact with the silica host. Furthermore, the confined space in as-prepared mesoporous silica has already been employed to accommodate amines to fabricate CO_2 capturer.[5] And our results from TG (Fig. 3) and N_2 adsorption (Fig. S16) could provide direct evidences for the successful introduction of guest to confined space. As shown in Fig. S16, some uptake and hysteresis can be observed in the isotherm of as-prepared SBA-15, due to the existence of space between template and silica walls. A hysteresis at low pressures emerges after the introduction of Ce precursor, and augments with the increase of Ce content. Moreover, the pore size decreases due to Ce loading. This gives evidence that Ce was assembled in the confined space. Otherwise, the overall N_2 uptake might decrease due to Ce introduction while neither the shape of isotherm nor pore size would change.

Most CeO_2 should be dispersed on the internal surface of mesoporous silica rather than other places. For mesoporous silica, most of the surface area (92-96%, varied with synthetic conditions) is derived from the internal surface.[9] If guest could not disperse on the internal surface, aggregation is difficult to avoid. To clarify this point, a mechanical mixture of CeO_2 and SBA-15 was prepared and denoted as 1.5CeO_2-SBA-15. The Ce content in this sample is identical to 1.5CeAS and 1.5CeCS, while CeO_2 is impossible to disperse on the internal surface. We performed XRD and UV-vis analysis for these three samples. As shown in Fig. S9, only a broad diffraction line center at 23^{o} originated from amorphous silica can be observed on 1.5CeAS and 1.5CeCS samples. However, the diffraction lines ascribed to CeO_2 (JCPDS No. 34-394) become visible on the reference sample 1.5CeO_2-SBA-15, indicating the aggregation of CeO_2. UV-vis spectroscopy provides a more sensitive approach to characterize CeO_2 dispersion. The absorption intensity decreases in the order of 1.5CeAS > 1.5CeCS > 1.5CeO_2-SBA-15, and the wavelength increases in the same order. That means, 1.5CeAS has the best CeO_2 dispersion, while CeO_2 aggregation takes place on 1.5CeO_2-SBA-15.

Competitive Adsorption.

As shown in Fig. S15, the adsorption ability of all samples decreased after the introduction of aromatic. Further calculation indicates that the decreased magnitude is 39% for CeAS while more than 50% for SBA-15 and CuCl/SBA-15. Similar results were also reported by other groups, and the adsorption capacity can be reduced by 50-75% due to the introduction of aromatics. Yang's group[10] investigated the desulfurization of transportation fuels by using the zeolite CuY. The saturation adsorption capacity was reduced by 65% in the presence of aromatic. Bu *et al.*[11] studied the adsorption of 4,6-dimethyldibenzothiophene (DMDBT) with activated carbons. They found that the presence of aromatic hydrocarbon can decrease the adsorption amount to a half. The results of Dai *et al.* indicated that the introduction of benzene can lead to a 75% decrease of adsorption amount.[5] This implies that aromatics can reduce sulfur compounds adsorption seriously. It is worth noting that our CeAS adsorbents can also capture a considerable amount of thiophene in the presence of aromatic, which is obviously higher than the typical adsorbent CuCl/SBA-15.

Aromatic sulfur compounds have two pairs of electrons on the sulfur atom. Accordingly, they can function either as a π-type donor by using the delocalized electrons of the aromatic ring to form a π-complex with a metal ion, or as an n-type donor by donating the lone pair of electrons of the sulfur atom to the adsorbent (direct S–M bond). Unlike Cu(I) and Ag(I), Ce(IV) is an f block element with a high positive charge and has a low trend to form π-complexes with π-bonding ligands.[12] Hence, the sulfur compounds are adsorbed over Ce(IV) by direct S–M interaction.

References

1 D. Zhao, J. Feng, Q. Huo, N. Melosh, G. H. Fredrickson, B. F. Chmelka and G. D. Stucky, *Science*, 1998, **279**, 548.

2 F. Kleitz, W. Schmidt and F. Schüth, *Microporous Mesoporous Mater.*, 2003, **65**, 1.

3 Y. Wang, R. T. Yang and J. M. Heinzel, *Chem. Eng. Sci.*, 2008, **63**, 356.

4 G.-S. He, L.-B. Sun, X.-L. Song, X.-Q. Liu, Y. Yin and Y.-C. Wang, *Energy Fuels*, 2011, **25**, 3506.

5 M. B. Yue, Y. Chun, Y. Cao, X. Dong and J. H. Zhu, *Adv. Funct. Mater.*, 2006, **16**, 1717.

6 W. Dai, Y. Zhou, S. Li, W. Li, W. Su, Y. Sun and L. Zhou, *Ind. Eng. Chem. Res.*, 2006, **45**, 7892.

7 Y. M. Wang, Z. Ying Wu and J. H. Zhu, *J. Solid State Chem.*, 2004, **177**, 3815.

8 A. Corma and H. Garcia, *Eur. J. Inorg. Chem.*, 2004, **2004**, 1143.

9 M. Kruk, M. Jaroniec, C. H. Ko and R. Ryoo, *Chem. Mater.*, 2000, **12**, 1961.

10 A. J. Hernández-Maldonado and R. T. Yang, *Ind. Eng. Chem. Res.*, 2002, **42**, 123.

11 J. Bu, G. Loh, C. G. Gwie, S. Dewiyanti, M. Tasrif and A. Borgna, *Chem. Eng. J.*, 2011, **166**, 207.

12 S. Velu, X. Ma and C. Song, *Ind. Eng. Chem. Res.*, 2003, **42**, 5293.

Table S1. Structural Parameters Calculated from N_2 Adsorption and Low-angle XRD Patterns

Sample	S_{BET} [a] ($m^2 \cdot g^{-1}$)	V_p [a] ($cm^3 \cdot g^{-1}$)	D_p [a] (nm)	a_0 [b] (nm)
SBA-15 [c]	–	–	–	11.6
SBA-15	725	1.19	8.7	10.6
0.5CeAS	709	1.17	8.8	12.2
1.0CeAS	663	1.12	8.9	12.2
1.5CeAS	645	1.11	8.9	12.4
2.0CeAS	639	1.10	8.9	12.1
3.0CeAS	586	1.02	8.5	12.1
0.5CeCS	645	1.06	8.4	11.9
1.0CeCS	630	1.02	8.4	11.9
1.5CeCS	590	0.96	8.4	11.9
2.0CeCS	573	0.93	8.4	11.9
3.0CeCS	535	0.87	8.4	11.9

[a] The Brunauer-Emmett-Teller (BET) surface area was calculated using the adsorption data in a relative pressure ranging from 0.04 to 0.2. The total pore volume was determined from the amount adsorbed at a relative pressure of about 0.99. The pore sizes were calculated using the Barrett-Joyner-Halenda (BJH) method. [b] Unit cell constant calculated according to $a_0 = 2 \times 3^{-1/2} \times d_{100}$. [c] As-prepared sample.

Table S2. Adsorption Capacity of Parent SBA-15, CeAS, and CeCS on Thiophene

Adsorbent	Adsorption capacity	
	mmol S/g adsorbent [a]	mol S/mol metal [b]
SBA-15	0.105	–
0.5CeAS	0.169	0.79
1.0CeAS	0.185	0.51
1.5CeAS	0.200	0.41
2.0CeAS	0.180	0.25
3.0CeAS	0.162	0.14
0.5CeCS	0.118	0.17
1.0CeCS	0.123	0.13
1.5CeCS	0.131	0.12
2.0CeCS	0.116	0.05
3.0CeCS	0.114	0.04

[a] Sulfur uptakes calculated from the breakthrough experiments at saturation. [b] Ratio of sulfur on metal calculated by subtracting the uptake of SBA-15 support from Ce-containing samples and then dividing by the amount of metal.

Table S3. Measured and Calculated Structural Parameters of Samples before Calcination

Sample	S_{BET} [a] ($\mathrm{m^2 \cdot g^{-1}}$)	V_{p} [a] ($\mathrm{cm^3 \cdot g^{-1}}$)	D_{p} [a] (nm)	V_{p} [b] ($\mathrm{cm^3 \cdot g^{-1}}$)
SBA-15	90	0.236	8.1	–
1.5CeAS	79	0.203	7.8	0.213
3.0CeAS	62	0.160	7.1	0.194

[a] BET surface areas, pore volumes, and pore sizes calculated from isotherms. [b] Pore volume calculated by assuming that $Ce(NO_3)_3$ located outside the pores rather than between template and silica walls.

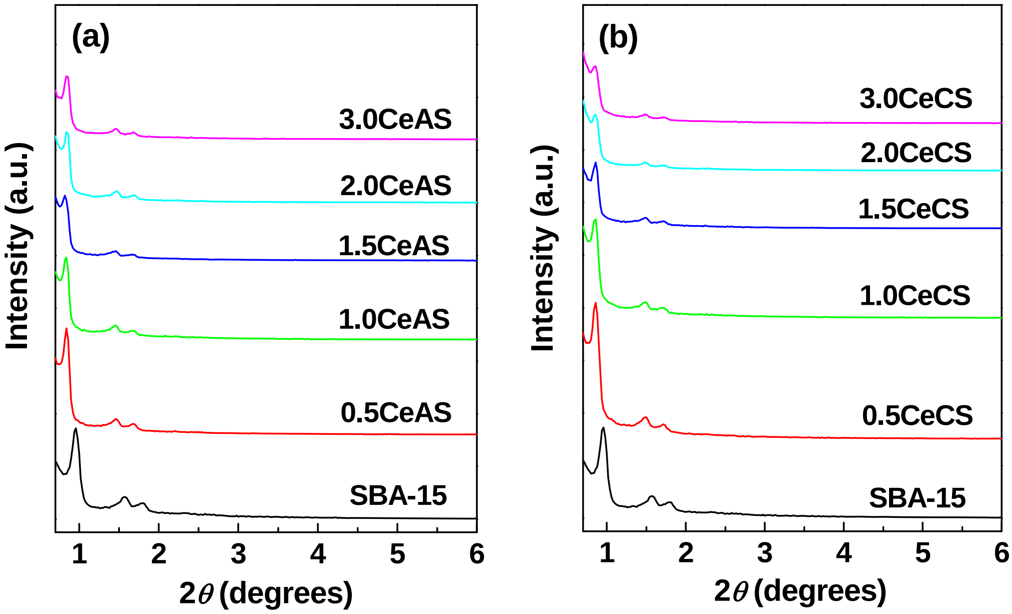

Figure S1. Low-angle XRD patterns of parent SBA-15, CeAS, and CeCS samples.

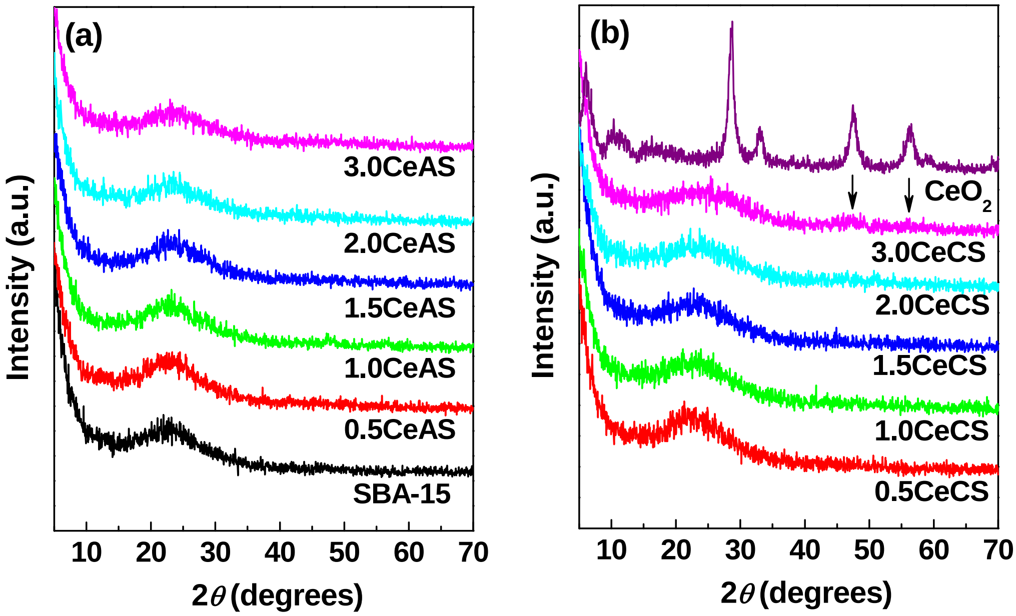

Figure S2. Wide-angle XRD patterns of parent SBA-15, CeAS, CeCS, and CeO_2 samples.

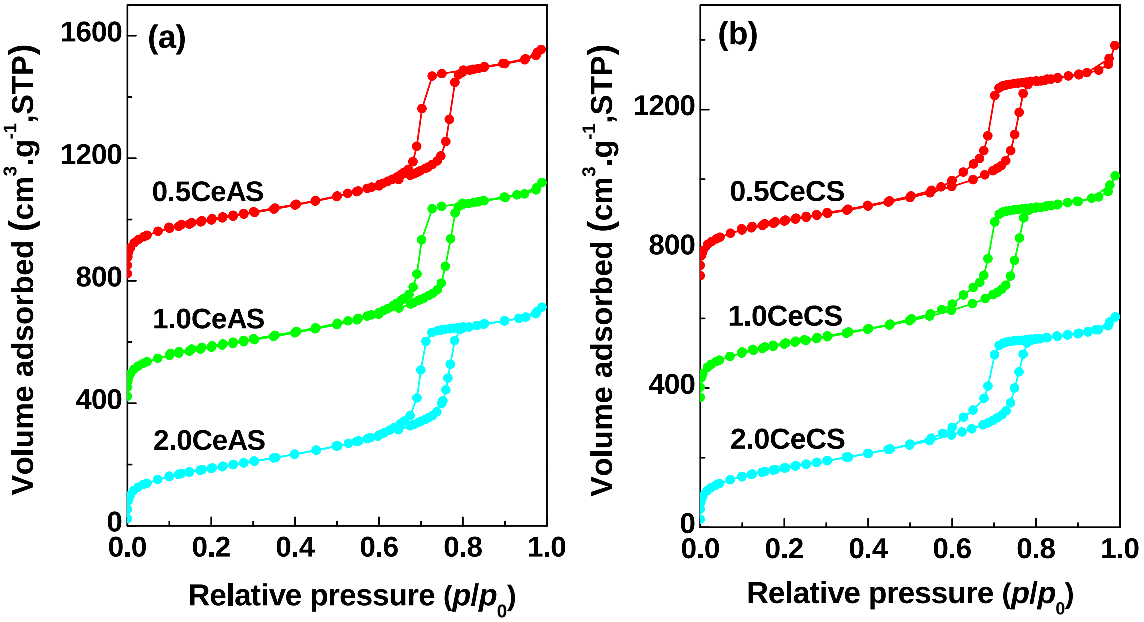

Figure S3. N_2 adsorption-desorption isotherms of CeAS and CeCS samples with different Ce content.

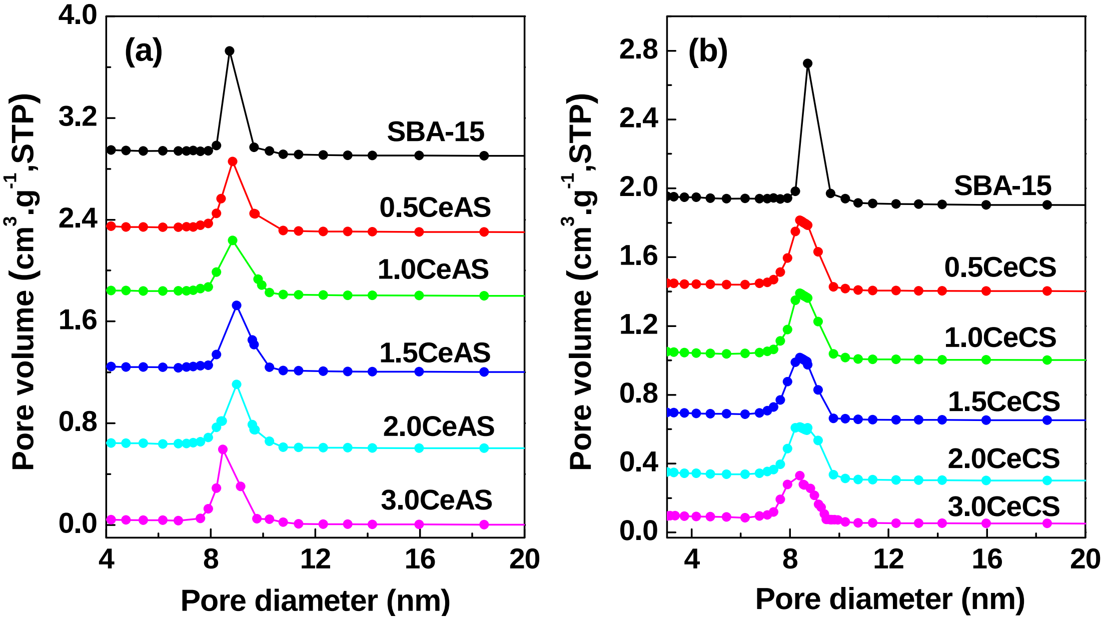

Figure S4. Pore size distributions of parent SBA-15, CeAS, and CeCS samples calculated from the adsorption branches.

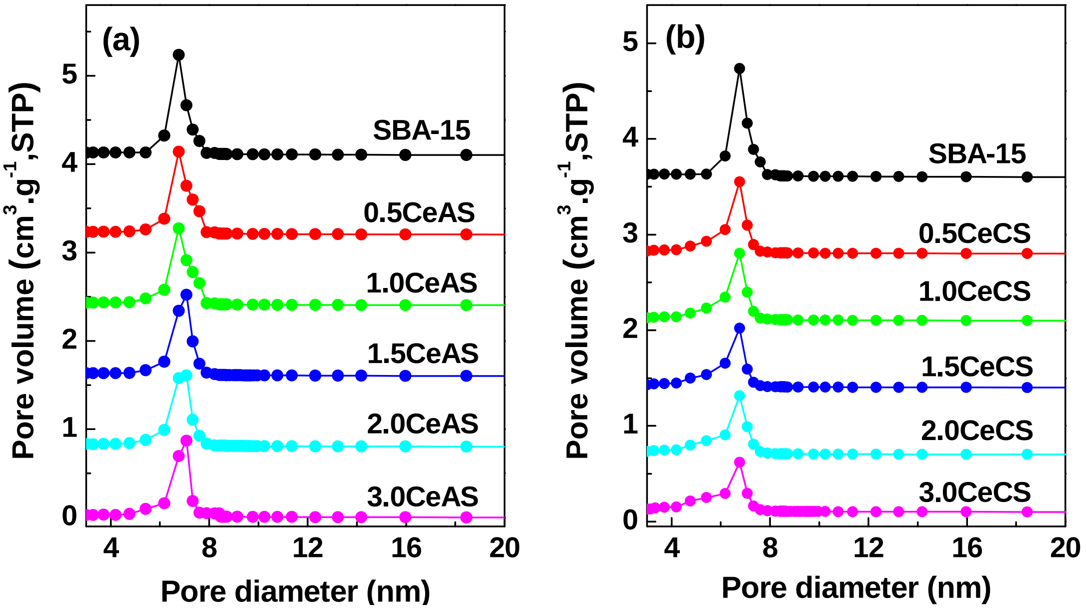

Figure S5. Pore size distributions of parent SBA-15, CeAS, and CeCS samples calculated from the desorption branches.

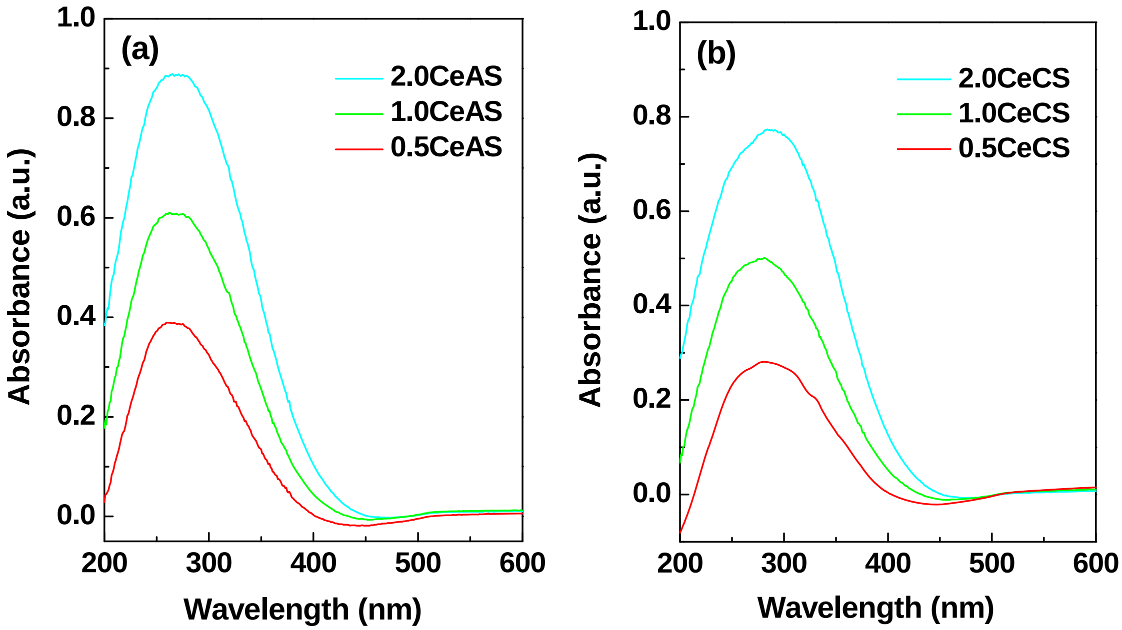

Figure S6. UV-vis spectra of CeAS and CeCS samples with different content of Ce.

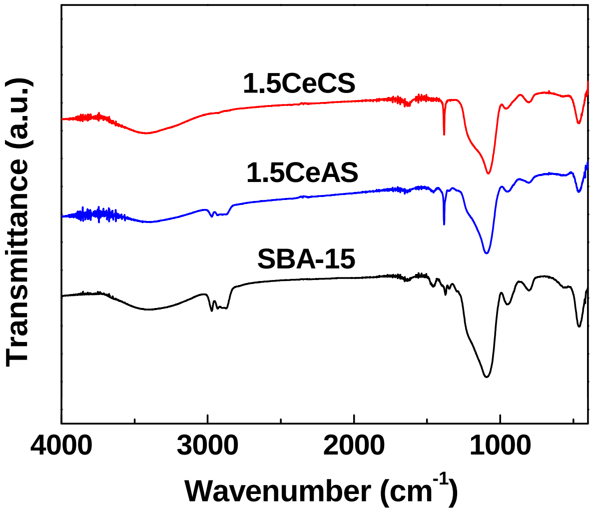

Figure S7. IR spectra of SBA-15, 1.5CeAS, and 1.5CeCS samples before calcination.

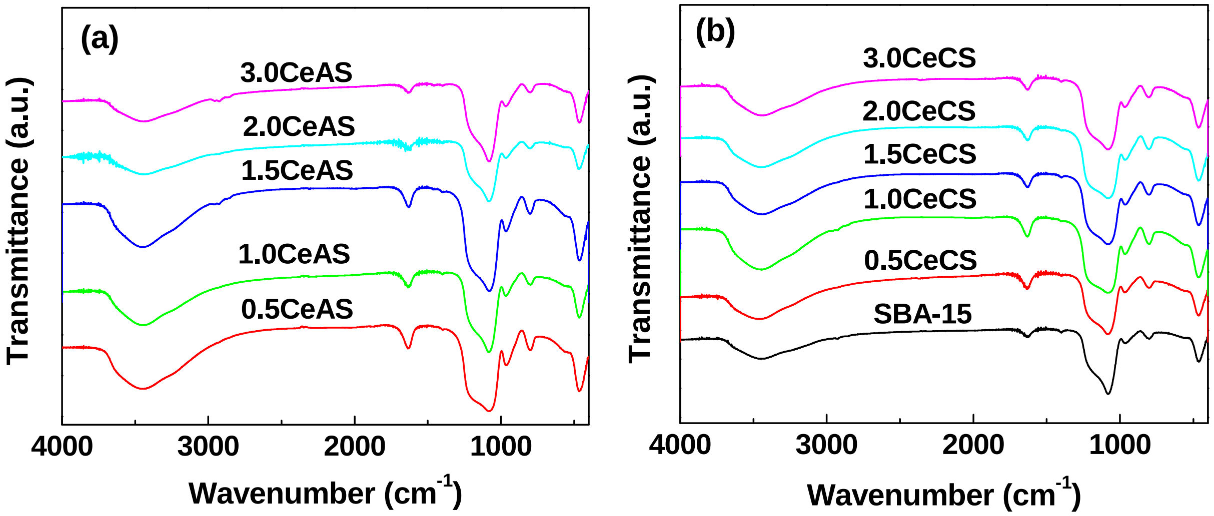

Figure S8. IR spectra of SBA-15, CeAS, and CeCS samples with different Ce content.

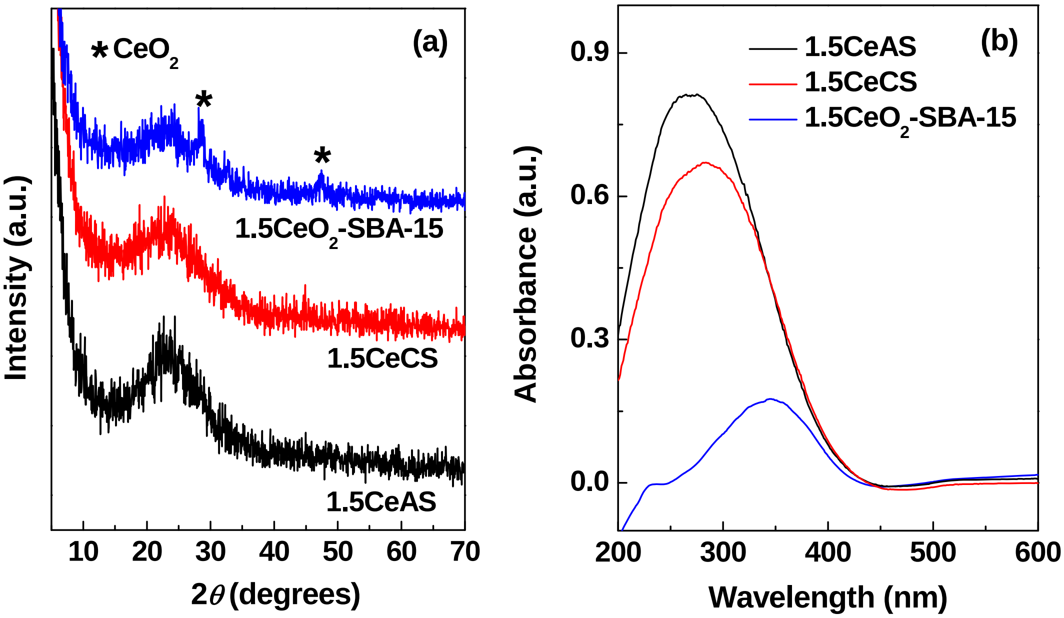

Figure S9. (a) Wide-angle XRD patterns and (b) diffuse reflectance UV-vis spectra of 1.5CeAS, 1.5CeCS, and 1.5CeO$_2$-SBA-15. The reference sample 1.5CeO$_2$-SBA-15 was prepared by grinding CeO$_2$ with SBA-15. The three samples possess the same Ce content.

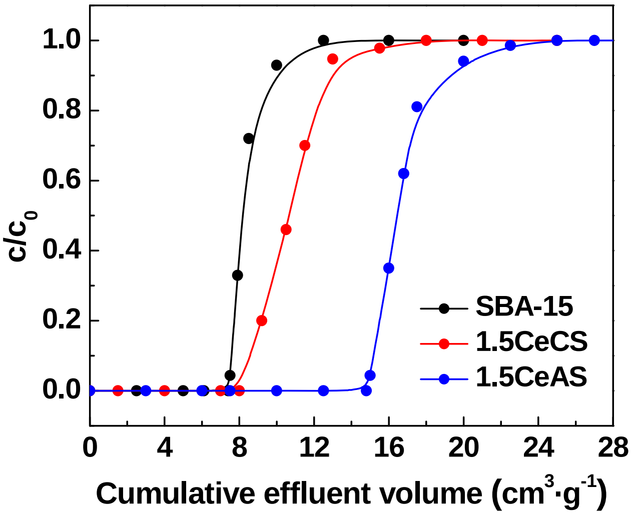

Figure S10. Breakthrough curves of thiophene in a fixed-bed adsorber with parent SBA-15, CeAS, and CeCS samples.

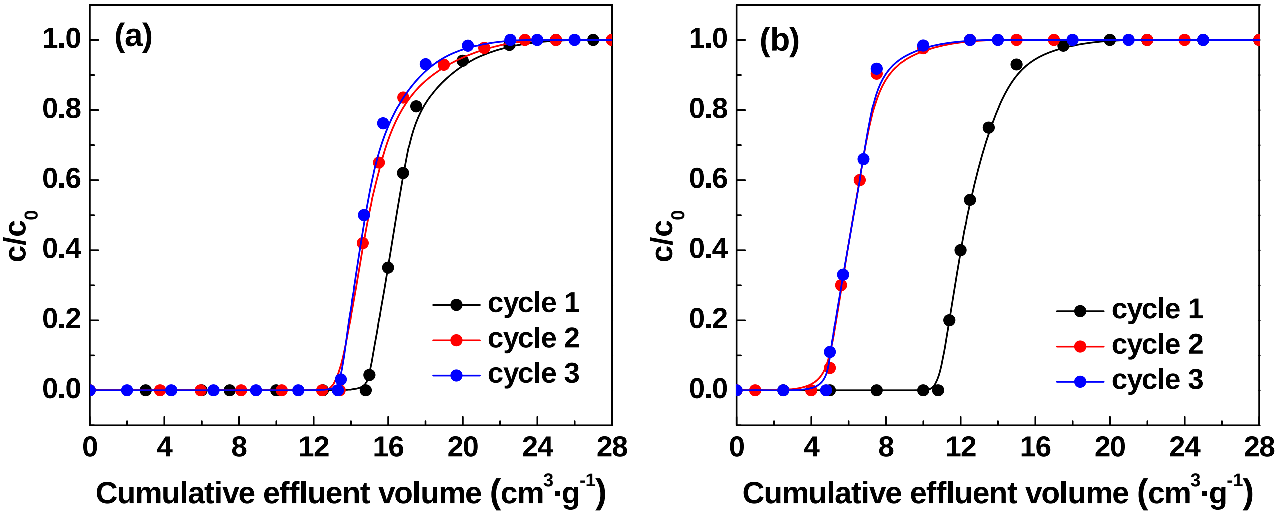

Figure S11. Breakthrough curves of thiophene in a fixed-bed adsorber with (a) 1.5CeAS and (b) CuCl/SBA-15 samples for three cycles.

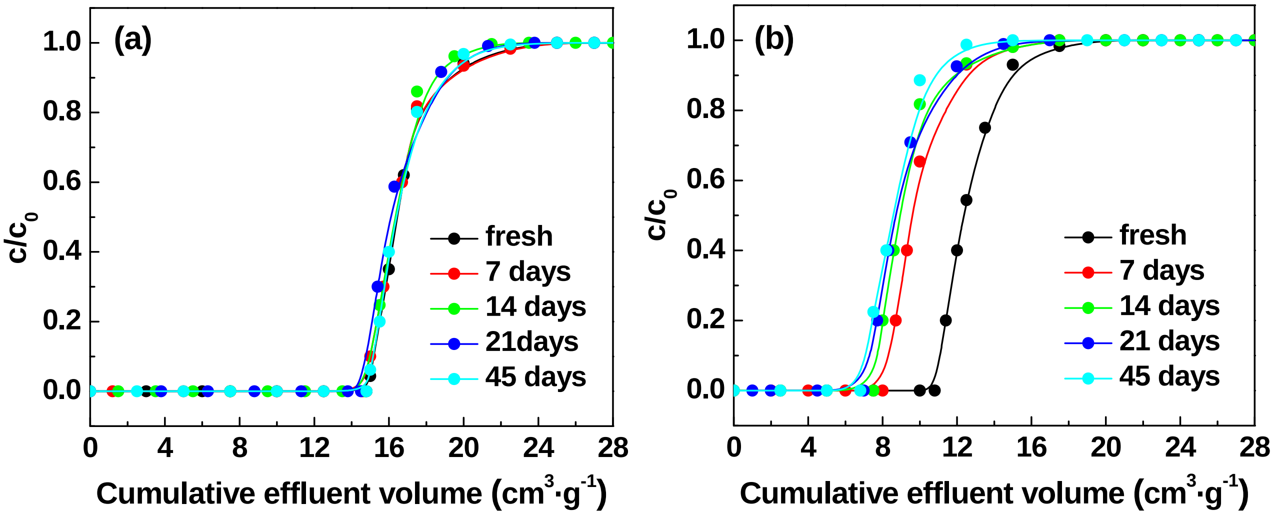

Figure S12. Breakthrough curves of thiophene in a fixed-bed adsorber with (a) 1.5CeAS and (b) CuCl/SBA-15 samples exposed to ambient conditions for different times.

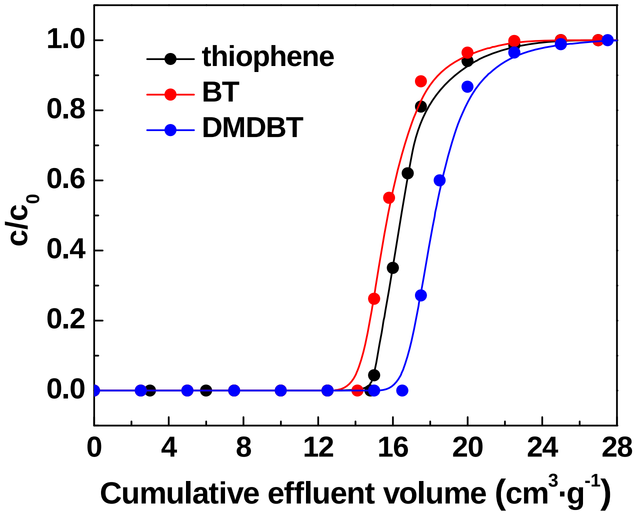

Figure S13. Breakthrough curves of different aromatic sulfur compounds, namely thiophene, BT, and DMDBT, in a fixed-bed adsorber with 1.5CeAS sample.

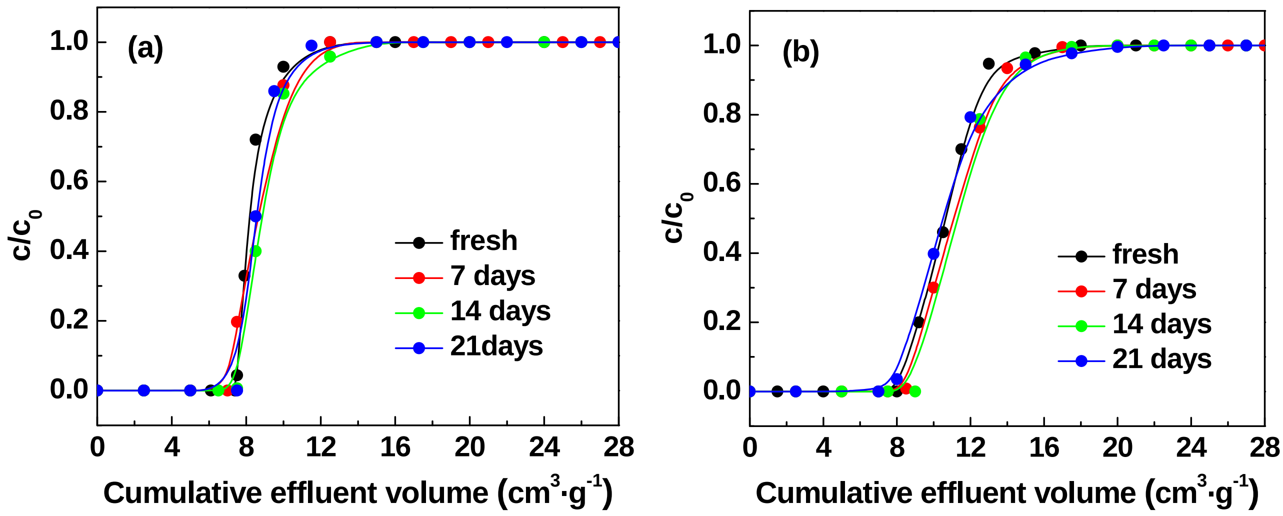

Figure S14. Breakthrough curves of thiophene in a fixed-bed adsorber with (a) SBA-15 and (b) 1.5CeCS samples exposed to ambient conditions for different times.

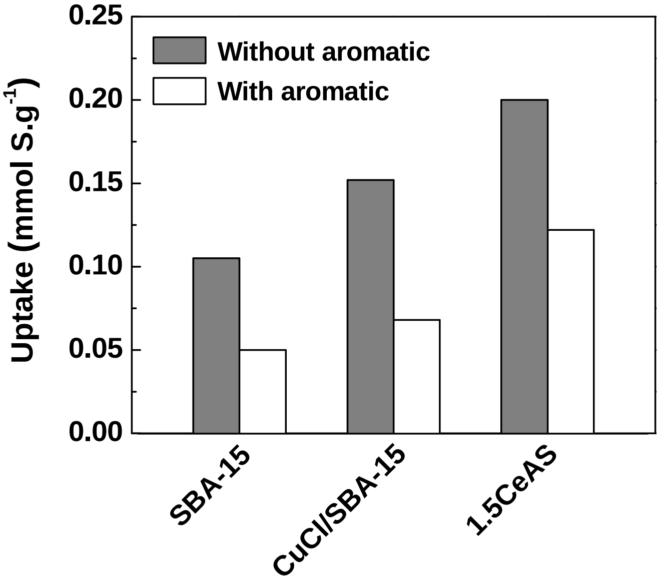

Figure S15. Adsorptive desulfurization performance of SBA-15, CuCl/SBA-15, and 1.5CeAS in the presence of aromatics.

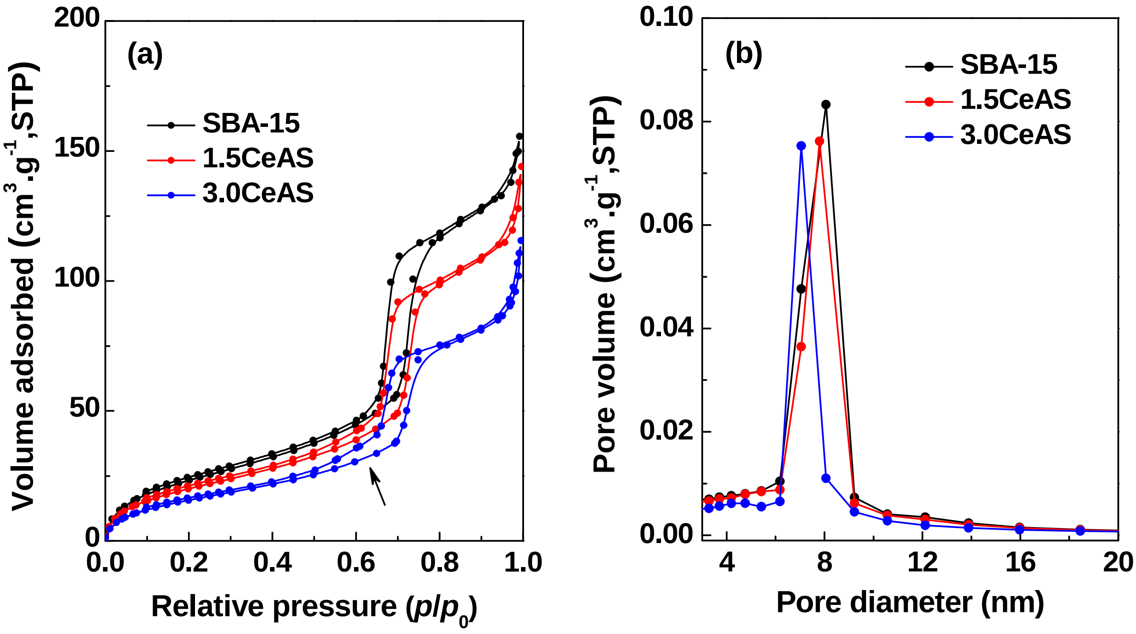

Figure S16. (a) N_2 adsorption-desorption isotherms and (b) pore size distributions of SBA-15, 1.5CeAS, and 3.0CeAS before calcination.